A Robust Control Design Framework for Substructure Models*

Kyong B. Lim†
NASA Langley Research Center
Hampton, Virginia

SUMMARY

A framework for designing control systems directly from substructure models and uncertainties is proposed. The technique is based on combining a set of substructure robust control problems by an interface stiffness matrix which appears as a constant gain feedback. Variations of uncertainties in the interface stiffness are treated as a parametric uncertainty. It is shown that multivariable robust control can be applied to generate centralized or decentralized controllers that guarantee performance with respect to uncertainties in the interface stiffness, reduced component modes and external disturbances. The technique is particularly suited for large, complex, and weakly coupled flexible structures.

1 Introduction

1.1 Problem Motivation

The motivation for studying this problem can be explained by considering the docking of the Shuttle with a space station as shown in figure 1. For the purpose

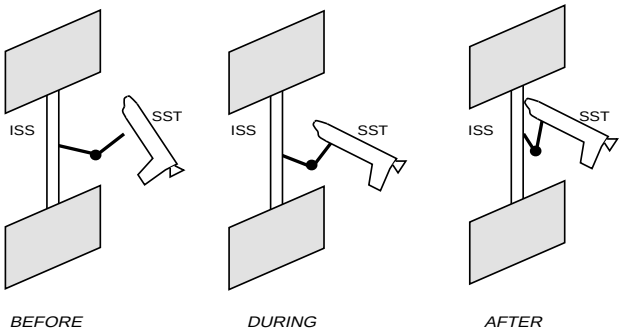

Figure 1: Docking/berthing of Shuttle and Station

of this study, we define the process of stiffness coupling between the Space Shuttle and station as docking. It should be noted that the coupling process is much more complicated than is assumed in this study, see for example reference [1, 2, 3]. During docking or joining of structures in space, a significant problem to be considered is the stabilization of the coupled system before, during, and after the docking of the two systems. An additional complication faced by the engineer is the difficulty in accurately predicting the dynamics of the coupled system because of the complexity in the physics of the interface or docking mechanism.

A further motivation for this work arises from the peculiar problem faced by the engineer in the development and validation of design models for a large flexible structure such as the space station. Due to the 1-g testing environment, it may not be possible to test the assembled structure on the ground so that only components can be tested. This means that only models of substructures can be refined directly using experimental data. However, component testing can be used to develop substructure uncertainty models arising from inadequate or incomplete component modes and inconsistencies in the substructure boundary conditions.

1.2 Relation to Previous Work

From the viewpoint of large scale systems theory many relevant results exist. Early results in [4] derive conditions for the existence of robust decentralized controllers for a general linear, time-invariant, interconnected subsystems. The controllers are assumed decentralized in the sense of local output feedback structure. Stability robustness is considered but a quantitative treatment of robustness is not given. The extension in [5] of the existence conditions to large flexible space structures are for colocated sensors and actuators. The results are further relaxed in [6] so that collocated sensors and actuators are not necessary. The existence conditions are used to guide the choice of actuators and sensors needed which is then followed by parameter optimization to obtain controller gains. Another decentralized controller configuration which is closely related to the class of dissipative controllers are developed for large flexible space structures [7, 8]. The results in [9] incorporates subsystem disturbance/performance variables and modeling uncertainties for general interconnected system. Controller existence conditions are derived and a discussion of the effect of structured uncertainty on stability robustness is given. It is however not clear how optimal robust controllers can be obtained.

From the viewpoint of structural modeling, several recent methods for decentralized control of large flexible structures, that are based on finite-elements and component modes synthesis exists. A technique whereby substructure controllers for each structural components

*Original version appeared as AIAA Paper No: 94-1699

†Research Engineer, Guidance & Control Branch, Flight Dynamics & Control Division, k.b.lim@larc.nasa.gov

are independently designed and then synthesized is given in [10]. The independent substructure controller designs are dependent on approximating the interface boundary conditions and component modeling of its adjacent components. To improve the approximation, internal boundary motion is minimized by feedback control. This method in general do not guarantee nominal stability and the report cites robustness issues as a current research direction, clearly recognizing inevitable component modeling errors. A substructure controller synthesis technique is proposed in [11, 12] whereby the controller is an assembly of subcontroller designs based on individual uncoupled substructures. However, as in [10], closed-loop stability is not guaranteed when the substructures are connected. This is not unexpected because the interface stiffness coupling is not taken into account in the synthesis. More recently, a substructure-based controller design approach has been proposed [13]. The basic idea is to combine a set of optimal component controllers which are designed independently. Recognizing the influence of neighboring substructures, the substructure plant used in the control design is appended by a simplified model of neighboring substructure dynamics. While this approach is computationally efficient, closed-loop stability is not guaranteed in general. In summary, note that since all structural models or for that matter, since all mathematical models are approximations of real physical systems, controllers that guarantee robust stability have a clear advantage over controllers that do not.

Although the previous work just described by no means represent all pertinent past results in the open literature, several issues appear to remain unresolved. Among these that are addressed in this paper include: accounting for component modeling errors, variations and/or undermodeling or modeling errors in the substructure interface, and performance robustness. As will be evident, the proposed framework amounts to an integration of well established results in substructure modeling and recent advances in multivariable robust control. The advantages in this synergism include: (1) nominal model and uncertainties at the substructure level can be incorporated directly for control analysis and design, and (2) a class of problems involving variable stiffness coupling between various structural systems can be treated conveniently. This approach allows substructure (or component mode synthesis) dynamic models (see for example [14], [15], [16], [17]) to be used directly in the analysis and design of control systems. Perhaps the major advantage in the above approach is the reduction in the dependence on on-orbit system identification testing of the assembled structure by an easier and less costly testing of substructures on the ground.

1.3 Organization of Paper

Section 2 outlines briefly the dynamic model of substructures which is then used in section 3 to define the uncoupled substructure robust control problem (for simplicity sake the acronym SRCP will be used) in the framework of modern multivariable robust control. A novel element in sections 2 and 3 is the inclusion of substructure boundary forces/moments as external disturbances on the substructure, and the displacement and rotations at the substructure boundaries as substructure output variables. The nominal substructure model and the associated uncertainties are defined along with the input and output control variables for the substructure. In section 4, a model for stiffness coupling is introduced and substructure interface stiffness matrix is defined. This interface stiffness matrix can be viewed as a transfer function matrix which maps the displacements and rotations at the interface to the corresponding interface forces and moments. Section 4 shows how displacements and rotations at the interface can be realized into a block diagram form suitable for connecting subsystems. For the case where the substructure interface involves a variable and or unknown stiffness coupling, the interface conditions can be treated as a parametric uncertainty in a multivariable robust control framework. In principle, this interface block could be extended to include certain or uncertain dynamic models. In section 5, the control problem for the connected system is defined by connecting the SRCP using the substructure interface block. To demonstrate the utility of the ideas introduced in this paper, a sequence of control design examples involving controller designs for two connected flexible beams are outlined in section 6 and section 7 contains a few concluding remarks.

2 Substructure Model

The following formulation is discussed in more detail in [15, 16]. Let $M^{(i)}$ and $K^{(i)}$ denote the mass and stiffness matrices corresponding to the i-th substructure so that the finite element model is given by

$$M^{(i)}\ddot{\xi}^{(i)}+K^{(i)}\xi^{(i)} = D_u^{(i)}u^{(i)}+D_I^{(i)}g^{(i)}+D_r^{(i)}r^{(i)} \quad (1)$$

where $\xi^{(i)}$ denote the physical nodal displacement vector. For substructure i, the matrices $D_u^{(i)}$, $D_I^{(i)}$, and $D_r^{(i)}$, denote respectively the force/moment distribution matrix for control input $u^{(i)}$, the substructure interface input distribution matrix for interface forces/moments $g^{(i)}$, and the force/moment distribution matrix for external command and/or disturbances $r^{(i)}$. It is important to note that in component mode synthesis, the interface forces and moments are not included or carried through in the substructure equations because they are absorbed in the synthesis process as internal forces and moments. However, the explicit consideration of these internal variables at the substructure interfaces is a key ingredient in the SRCP formulation.

The substructure eigenvalue problem for substructure i, for an assumed set of boundary conditions, is given by

$$K^{(i)}\psi_j^{(i)} = \lambda_j M^{(i)}\psi_j^{(i)} \quad (2)$$

where j denotes the structural mode number. Using only a subset of substructure or component modes $\Psi^{(i)}$ where

$$\xi^{(i)} = \Psi^{(i)}\eta^{(i)} + \Psi_{tr}^{(i)}\eta^{(i)} \quad (3)$$

the Ritz approximation leads to the substructure reduced modal model,

$$\begin{aligned}\ddot{\eta}^{(i)} + \Omega^{(i)^2}\eta^{(i)} &= \Psi^{(i)T}D_u^{(i)}u^{(i)} + \Psi^{(i)T}D_I^{(i)}g^{(i)} \\ &+ \Psi^{(i)T}D_r^{(i)}r^{(i)} \quad (4)\end{aligned}$$

where $\eta^{(i)}$ is the modal amplitude vector, and $\Omega^{(i)^2} = diag(\omega_1^{(i)^2}, \ldots, \omega_n^{(i)^2})$. The columns of $\Psi_{tr}^{(i)}$ denote truncated modeshapes for substructure i.

In general, the synthesized component modes model do not lead to a model with sufficient fidelity when only the truncated sets of "normal" component modes (represented by $\Psi^{(i)}$ in Eq.(3)) are used in the synthesis. Therefore, the reduced set of "normal" component modes are typically augmented with "constraint" modes. For a more comprehensive treatment on adding constraint modes to normal modes, the textbook [15] is recommended. Indeed, the selection of a subset of component modes or assumed shape functions is an important element in substructure synthesis and the work in [17, 13] is recommended for a more detail discussion.

In the sections to follow, the effect of the truncated substructure modes, $\Psi_{tr}^{(i)}\eta^{(i)}$ in Eq.(3) (i.e. the Ritz approximation error), are included as additive uncertainties about the nominal model. The closed-loop robustness is partly with respect to this model error. It is significant to note that if the entire set of component modes span the entire substructure configuration vector space, a Ritz approximation plus the additive uncertainty will be sufficient to span this vector space. An implication of this truth is that potential spillover into the truncated modes can be properly accounted for in the control design although closed-loop performance is limited by the inaccurate set of reduced normal modes.

The displacement and velocity outputs for substructure i are given by

$$y^{(i)} = \begin{Bmatrix} y_d^{(i)} \\ y_v^{(i)} \end{Bmatrix} = \begin{bmatrix} D_d^{(i)T}\xi^{(i)} \\ D_v^{(i)T}\dot{\xi}^{(i)} \end{bmatrix} \quad (5)$$

$$\approx \begin{bmatrix} D_d^{(i)T}\Psi^{(i)} & \\ & D_v^{(i)T}\Psi^{(i)} \end{bmatrix} \begin{Bmatrix} \eta^{(i)} \\ \dot{\eta}^{(i)} \end{Bmatrix} \quad (6)$$

The displacement and rotation at the interface for substructure i are

$$\xi_b^{(i)} = D_b^{(i)T}\xi^{(i)} \quad (7)$$

$$\approx D_b^{(i)T}\Psi^{(i)}\eta^{(i)} \quad (8)$$

Each column of $D_b^{(i)}$ corresponds to the individual interface degree of freedom (DOF) location for substructure i. The outputs of interest are written as

$$e^{(i)} = \begin{bmatrix} D_{e_d}^{(i)T} & D_{e_v}^{(i)T} \end{bmatrix} \begin{Bmatrix} \xi^{(i)} \\ \dot{\xi}^{(i)} \end{Bmatrix} \quad (9)$$

$$\approx \begin{bmatrix} D_{e_d}^{(i)T}\Psi^{(i)} & D_{e_v}^{(i)T}\Psi^{(i)} \end{bmatrix} \begin{Bmatrix} \eta^{(i)} \\ \dot{\eta}^{(i)} \end{Bmatrix} \quad (10)$$

In the field of structural dynamics, the main purpose of substructure modeling via component mode synthesis appears to be the prediction of frequencies and modeshapes and possibly damping for the assembled structure. The modular nature of this approach also allows independent structural analysis and refinement and component testing even by separate organizations. Although much attention has been given to the basic problem of component mode selection, issues pertaining to the use of substructure models for controller design has not been fully addressed. As a result, two problems that are addressed in this study are substructure model reduction errors and the modeling of variable or uncertain substructure interface both in the context of performance robustness of closed-loop coupled substructures.

3 Uncoupled SRCP

Define the states for substructure i as

$$x^{(i)} = \begin{pmatrix} \eta_1^{(i)} & \dot{\eta}_1^{(i)} & \ldots & \eta_n^{(i)} & \dot{\eta}_n^{(i)} \end{pmatrix}^T \quad (11)$$

The substructure state equations can be written as

$$\dot{x}^{(i)} = A^{(i)}x^{(i)} + B_1^{(i)}g^{(i)} + B_2^{(i)}r^{(i)} + B_3^{(i)}u^{(i)} \quad (12)$$

The coefficient matrices, $B_1^{(i)}$, $B_2^{(i)}$, and $B_3^{(i)}$, are state space forms of $D_u^{(i)}$, $D_I^{(i)}$, and $D_r^{(i)}$, in Eq.(1). The displacement measurement, pointing error, and interface boundary DOF can be written in terms of substructure state vector,

$$y^{(i)} = C_3^{(i)}x^{(i)} \quad (13)$$

$$e^{(i)} = C_2^{(i)}x^{(i)} \quad (14)$$

$$\xi_b^{(i)} = C_1^{(i)}x^{(i)} \equiv z_i \quad (15)$$

Similarly, the coefficient matrices, $C_3^{(i)}$, $C_2^{(i)}$, and $C_1^{(i)}$, are the corresponding state space forms of the relevant outputs in Eqs.(5) to (10). Denote the transfer function matrix of substructure i as

$$G^{(i)} = \begin{bmatrix} A^{(i)} & B^{(i)} \\ C^{(i)} & 0 \end{bmatrix} \quad (16)$$

where

$$B^{(i)} = \begin{bmatrix} B_1^{(i)} & B_2^{(i)} & B_3^{(i)} \end{bmatrix}; C^{(i)} = \begin{bmatrix} C_1^{(i)} \\ C_2^{(i)} \\ C_3^{(i)} \end{bmatrix} \quad (17)$$

The transfer function matrix of the substructure, $G^{(i)}$, is then appended with weighting matrices that define substructure closed-loop performance and uncertainties peculiar to that substructure to form augmented substructure plant, $P_{(i)}$.

For the special case where the substructures are uncoupled (for example at the onset of docking), Figure 2 shows the subsystem plants, P_1 and P_2, substructure controllers, k_1 and k_2, and uncertainties associated with each substructure, Δ_1 and Δ_2. Although the following development is based on a system with only two substructures, it should be clear that the methodology presented applies also to a system with arbitrary number of substructures. The subsystem plants consist of substructure models which are augmented with performance, disturbance and uncertainty weighting matrices that are used to define the substructure control problem. The uncertainty blocks are assumed to be normalized to unity in terms of their maximum singular values (see for example [18]). The structure in the uncertainty block is problem dependent and is selected by the engineer.

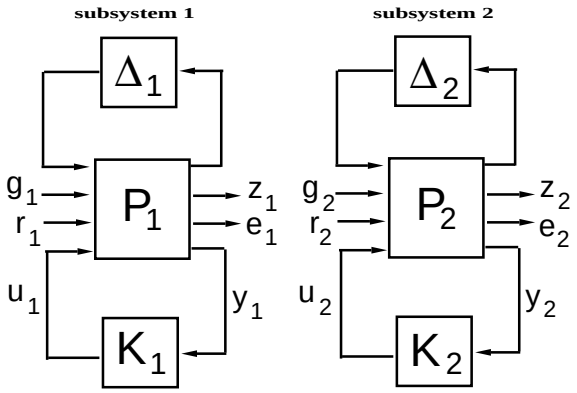

Figure 2: Uncoupled SRCP for two substructures

The uncoupled SRCP can be described as seeking a controller $k_{(i)}$ which maintains stability and performance for the set of all closed-loop systems defined by the given uncertainty set Δ_i. The performance considered is defined in terms of a frequency weighted H_∞ norm, of the transfer function matrix from the disturbances, r_1, r_2 to outputs of interest e_1, e_2. The above form of the performance can physically represent regulation, tracking, and/or disturbance rejection problems.

In general, any suitable multivariable design approach can be used to generate a substructure robust controller. References [7, 19] describe several control design approach including parameter optimization via nonlinear programming. In this paper, we consider the robust performance measure in terms of the structured singular value. The problem then reduces to minimizing μ (see for example [20, 21, 22, 23]).

4 Substructure Interface

In this section, a model of a substructure interface is developed for the purpose of formulating the coupled SRCP.

4.1 Static Interface

Consider the structural interconnection between two substructures. Denote those DOF at the interface boundaries for the two substructures by superscripts $^{(1)}$ and $^{(2)}$, and the stiffness interfaces denoted by superscript $^{(I)}$. The variables $\xi^{(1)}_{b1}, ..., \xi^{(1)}_{bm}$ denote the DOF at the interface for substructure 1 while $\xi^{I/(1)}_{b1}, ..., \xi^{I/(1)}_{bm}$ denotes the structural interface DOF adjoining substructure 1. Similarly, the variables $\xi^{(2)}_{b1}, ..., \xi^{(2)}_{bm}$ correspond to the DOF at the interface for substructure 2 while $\xi^{I/(2)}_{b1}, ..., \xi^{I/(2)}_{bm}$ denotes the DOF at the adjoining interface structure. The interface stiffness matrix, S^I, is defined as follows

$$S^I \left\{ \begin{array}{c} \xi^{I/(1)} \\ \xi^{I/(2)} \end{array} \right\} = \left\{ \begin{array}{c} f^{I/(1)} \\ f^{I/(2)} \end{array} \right\} \tag{18}$$

where all the variables without subscripts denote vector representation of corresponding DOF. As in any stiffness matrtix, the (i,j)th element of S^I physically represents the force (or moment) at DOF i due to a unit displacement (or rotation) at DOF j. In the general case where there are DOF internal to the interface substructure itself, the interface stiffness matrix in the boundary input/output form, as in Eq.(18), can be obtained by a static condensation procedure [24].

As an example of a static substructure interface, consider the attachment of a flexible aircraft wing to its fuselage as shown in figure 3. A narrow strip of

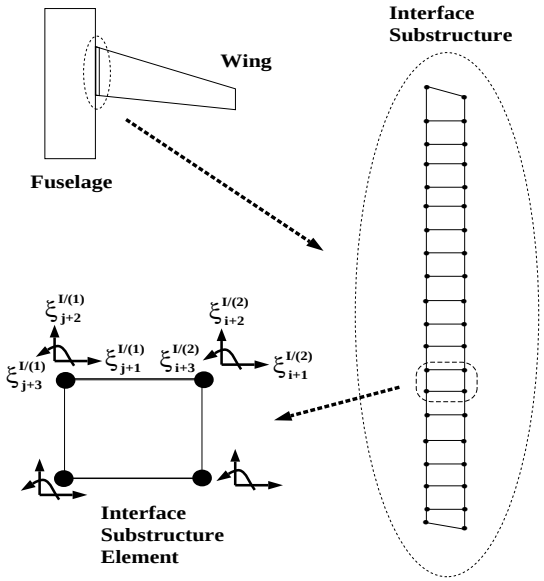

Figure 3: Structural interface between a wing and its fuselage.

structure located between the wing and the fuselage can be seperately modeled by finite-elements just as is done for the main substructures. $\xi^{I/(k)}_m$ denotes the mth finite-element DOF at the physical node shared by the substructure interface and kth substructure. The interface stiffness for this example relates the interface displacements, forces, and rotations, moments, in the same way as Eq.(18) if we let the superscripts, $^{(1)}$ and $^{(2)}$ denote the fuselage and wing respectively.

From a controls perspective, the interface stiffness can be viewed as a collocated, constant gain output feedback of the displacements and rotations at the substructure interface to the forces and moments on the same substructure interface. Figure 4 show this

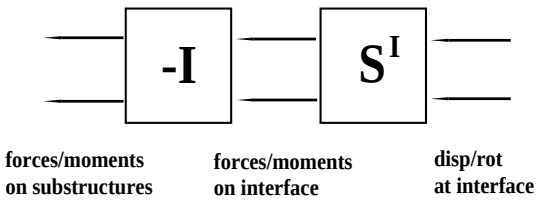

Figure 4: Substructure interface block diagram

constant gain feedback block given in terms of forces and moments on the substructures. Note that since the forces (and moments) in the right hand side of Eq.(18) are the forces (and moments) acting on the stiffness interface, the reaction forces (and moments) on the substructures will be in opposite directions.

4.2 Varying/Uncertain Interface

In the event that the substructure interface is uncertain and/or varying, the coupling block can be viewed as a constant linear uncertainty with specified norm bounds. One approach is to model the uncertainty as an independent variation in the interface forces about a nominal stiffness, s_o.

For stiffness interface let the variation in the interface stiffness be modeled by the following equation between the substructure boundary displacements (and rotations) $(\xi_b^{(1)}, \xi_b^{(2)})$, and the corresponding forces (and moments) (g_1, g_2) on the substructures at the boundaries

$$\begin{Bmatrix} g_1 \\ g_2 \end{Bmatrix} = s \begin{Bmatrix} \xi_b^{(1)} \\ \xi_b^{(2)} \end{Bmatrix} \tag{19}$$

where

$$s = -(\gamma + \beta\alpha) S^I \tag{20}$$

denotes the effective interface stiffness while α, β, γ are parameters which are defined as follows:

$$|\alpha_i| \leq 1; \qquad i = 1, \ldots, \#boundaryDOF \tag{21}$$

$$\beta_i = \alpha_i^u \tag{22}$$

The parameter γ is a factor appearing in the nominal interface stiffness

$$s_o = -\gamma S^I \tag{23}$$

Notice that when $\gamma = 0$ is selected, it means that the nominal interface stiffness is zero. However, this do not necessarily imply that the substructures are uncoupled. The combined term, $\beta\alpha$ denotes the factor of interface stiffness variation about the nominal. α_i^u denotes the upper limit of change in the ith channel. Note that the ith channel physically corresponds to the ith interface DOF. Figure 5 shows in block diagram

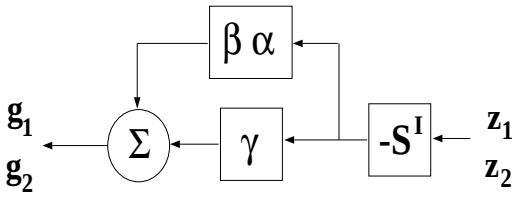

Figure 5: Interface stiffness uncertainty/variation

form the effective interface stiffness parameterized as a structured uncertainty.

4.3 Dynamic Interface

So far we assumed a static model in the form of a stiffness coupling and a substructure interface stiffness matrix is formally defined. In principal, the interface stiffness matrix can be extended to a transfer function matrix which maps the dynamic displacements and rotations at the interface to the corresponding interface forces and moments. In other words, an inverse kinematics model can be developed whereby the kinematic variables (displacements, velocities and accelerations) at the DOFs adjacent to the substructures are mapped into the corresponding forces and moments.

Similar to the static stiffness interface case, the dynamic interface block could be extended to include certain or uncertain dynamic models. As an example, the interface dynamics associated with a remote manipulator arm between the orbiter and the space station (figure 1) could be modeled as a flexible substructure with its own nominal model and uncertainty. More interestingly, it may be sufficient to treat the complex variations due to a slow configuration change in the manipulator arm during docking or when grabing a payload, as a set of plants not different from uncertainty descriptions.

5 Coupled SRCP

In this section, the substructure interface model is combined with the uncoupled SRCP to form a coupled SRCP. It is important to note that a single synthesized model is not formed by removing the interface DOF to predict system frequencies and mode shapes as is traditionally done in component modes synthesis (see for example [15, 16]).

The two substructures connected by a stiffness interface can be represented graphically in block diagram form as shown in figure 6. The control objective remains

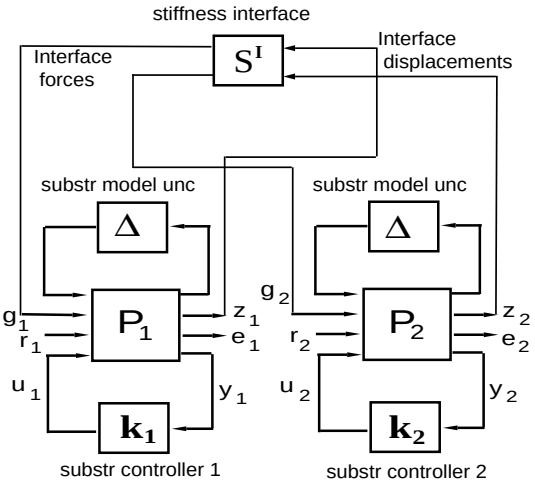

Figure 6: Stiffness coupled SRCP for two substructures.

the same as the uncoupled SRCP, i.e. to optimize disturbance rejection performance under substructure model uncertainties. However, the objective for coupled SRCP becomes more complicated due to the substructure coupling which may also be slowly varying and/or even uncertain. The disturbance rejection performance is in the form of a frequency weighted H_∞ norm, of the transfer function matrix from the disturbances, r_1, r_2 to outputs of interest e_1, e_2. The disturbance rejection performance is to be guaranteed under all modeled uncertainties.

Figure 7 shows a general interconnected substructures. The system plant, P, consists of nominal substructure models, P_1, P_2, ..., while the system uncertainty, Δ, consists of individual substructure uncertainties, Δ_1, Δ_2, ... The system controller, K, consists of substructure controllers, $k_1, k_2, \ldots$. A block-diagonal substructure interface however couples the nominal substructures, component uncertainties and

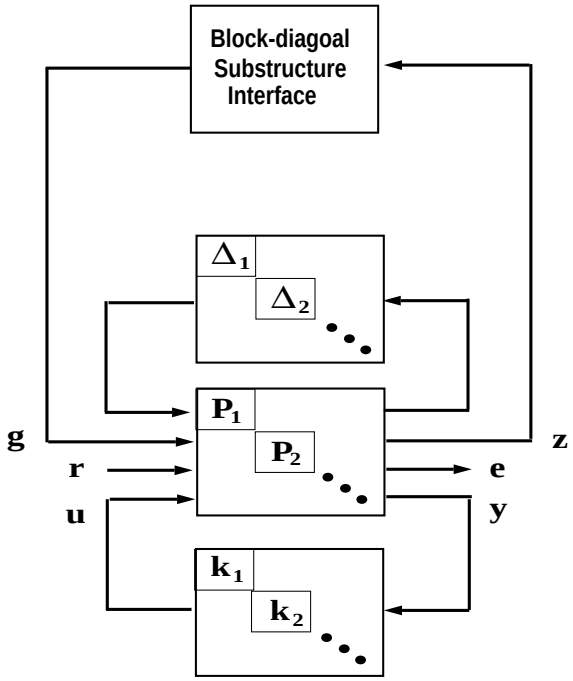

Figure 7: General Coupled SRCP.

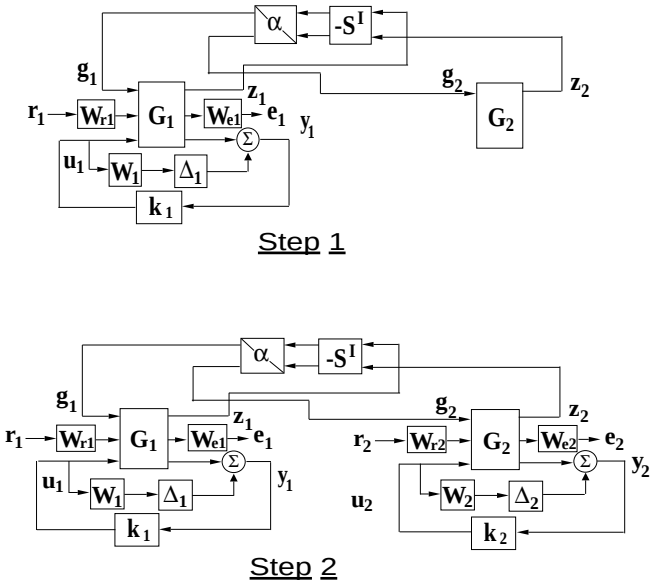

Figure 8: Design sequence for robust decentralization

substructure controllers. The width dimension of the block diagonality of interface coupling is dependent on the degree of physical coupling and topology of the interconnections. Notice that even if each of the substructure and interface uncertainties are unstructured, globally, the uncertainties will be highly structured. This is the basis for applying structured singular value techniques (see for example [20, 21, 22, 23]) for robust performance controller design in this study.

5.1 Decentralized Control

Figure 7 shows the decentralized nature of the plant, uncertainty, and controller. The decentralized controller structure (see for example [25, 26, 27]) is enforced by the classical loop-at-a-time design, namely, design a substructure controller while holding the remaining substructure controllers constant. Figure 8 shows the first two steps of the design sequence to incorporate both robustness and decentralization of the overall system for a system with two substructures.

The first step involves the design of substructure controller, k_1, while assuming open loop for substructure 2. At this step, the nominal dynamics of the substructure 2 is included while the component uncertainty and performance for the remaining substructure 2 are ignored. Ignoring the adjacent component's uncertainty and performance is crucial to obtain a reasonable performance controller for substructure 1 because of the localized constraint on substructure controller 1. Accounting for nominal substructure 2 should result in substructure controller 1 which takes into account the primary coupling effects of the neighboring substructure.

In the second step, the controller for substructure 2, k_2, is designed by holding the controller for substructure 1, k_1, constant. The fixed controller k_1 should strongly complement controller k_2 in the control of substructure 2. At this step, all uncertainties and disturbances with the corresponding errors are included. This essentially guarantees performance robustness of the overall system.

Step 3 is similar to step 2 except substructure controller 2 is held constant while substructure controller 1 is refined. Step 4 is the same as step 2 and the sequence follows. For this design example, iterations up to step 3 are carried out for the decentralized control design. In the sequential design process described above, the order of the controller will increase with each iteration if the control design technique chosen results in a controller of the same order as the current augmented plant (such as LQG or central H_∞). Hence, model order reduction is recommended after each step.

5.2 Design via μ Synthesis

The disturbance rejection performance from r to e in terms of frequency weighted H_∞ norm is to be guaranteed (or be robust) with respect to a bounded and structured set of component uncertainties, Δ_1, Δ_2, and interface uncertainty, Δ_s. The controller can be centralized or decentralized as outlined in the previous section. The worst case (over frequency) μ quantifies the degree of robust performance. Designing controllers by μ-synthesis involves an iterative minimization of the upper bound using H_∞ methods. The underlying theory which forms the basis of this method is discussed in detail in [23, 28, 29, 30].

The μ-design problem is summarized as follows:

$$\underset{K,D}{\text{minimize}} \ \|DF_l(P,K)D^{-1}\|_\infty \tag{24}$$

where $\{K : F_l(P,K) \in H_\infty\}$, $D \in \underline{D}$. The set of scaling matrices, $\underline{D}$, has a similar structure as $\underline{\Delta}$ (the structured uncertainty matrix) with an appended identity matrix. The terms, F_l, P, and K, denote the lower linear fractional transformation, augmented plant, and the controller, respectively. To minimize the weighted H_∞ norm in Eq. 24, the D-K iteration

technique is used. In this approach, D or K is optimized independently and sequentially. Optimizing for D while keeping K fixed involves the search for the minimal upper bound on μ, whereas, optimizing for K while fixing D involves the minimization of an approximation of μ itself. Although this approach is iterative in nature and convergence to a global minimum is not guaranteed, recent numerical studies show excellent convergence (see for example [21, 31, 32]). The Glover-Doyle algorithm [33, 34] is used to solve the H_∞ problem. The MATLAB toolbox, μ-Tools [22] is used for the analysis and synthesis of the controllers.

6 Example

6.1 Description of Structure

Motivated by earlier work on substructure and component mode synthesis, a beam which is cantilevered at both ends is used to illustrate the ideas introduced in this paper. The structure is assumed to consist of two cantilevered Euler-Bernoulli beams joined at the free ends by a short stiffness interface beam element as shown in figure 9.

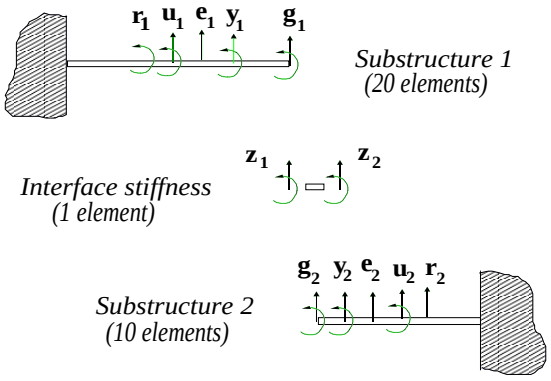

Figure 9: Joined cantilever beams

The structural properties and configurations of the beams are given in table 1. The stiffness and

Property	*Substr 1*	*Substr Inter*	*Substr 2*
length	2	.2	1
mass density (ρ)	10	.1	10
stiffness (EI)	10^{-2}	10^{-4}	10^{-2}
No. of elements	20	1	10

Table 1: Structural Properties and Configuration

mass density properties are selected such that the resonant frequencies are sufficiently spaced, and the lower frequencies to be controlled are sufficiently small to allow reasonable numerical integration. No deep significance should be attributed to the choice of the numerical values in table 1 since this is obviously a contrived example to clarify the proposed approach. The beam substructures modeled by 20 and 10 beam elements resulted in 40 and 20 structural modes. The full state space models of the two substructures are then of orders 80 and 40, respectively. The interface stiffness is modeled by a single beam element with four DOF.

The connected structure has 60 structural modes from the total of 31 beam elements. A truncated structural model consisting of the lowest 30 structural modes is used as the evaluation model and figure 10 show the maximum and minimum singular values of

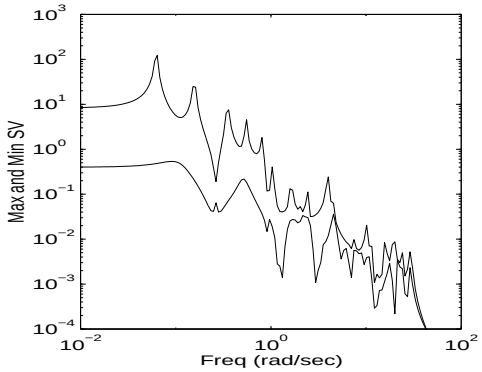

Figure 10: Frequency response of evaluation model

the frequency response matrix from r_1, r_2, to e_1, e_2. Notice that there is no clear frequency gap where model reduction by modal truncation can be done. It is also clear from the figure that the displacement responses rapidly drop as a function of frequency; this is the basis for modal truncation of higher frequency modes in addition to the well known inaccuracy of the finite element model in predicting the dynamics at higher frequencies.

6.2 Control Design

6.2.1 Objective

The control objective for this problem is to optimize disturbance rejection performance. In particular, a minimal desired upper bound of frequency weighted H_∞ norm, of the transfer function matrix from the disturbances, r_1, r_2 to outputs of interest e_1, e_2, is to be guaranteed under truncated component modes and uncertainties and/or variations in the substructure interface. To optimize the robust performance, μ synthesis is used.

6.2.2 Design Configuration

The overall system block diagram is shown in figure 11. The two nominal component modes model, (G_1,G_2), with their corresponding high frequency truncated modes which are treated as substructure uncertainties ($\Delta_1 W_1$, $\Delta_2 W_2$), are shown. The respective substructure disturbances, (r_1,r_1), and outputs of interests, (e_1,e_2), are also distinguished. The power spectrum of the disturbances are represented by W_{r_1}, and W_{r_2} which frequency weights the all-pass input disturbances. The output error weighting matrices, W_{e_1}, and W_{e_2} were chosen as unity but in general may be chosen to signify its relative importance with respect to other requirements. The unstructured uncertainty blocks, Δ_1, Δ_2, and diagonally structured interface stiffness uncertainty block $[\alpha]$, are assumed to be amplitude bounded by unity 2-norm. The interface stiffness

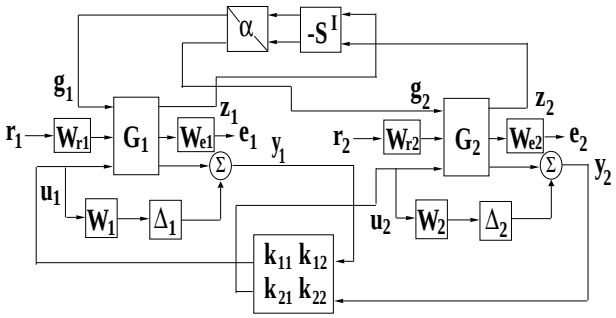

Figure 11: Block diagram for control design

block couples the substructures and acts like a constant gain feedback. The controller shown in figure 11 are centralized and are used for performance comparisons. Substructure decentralization is defined by $k_{12} = k_{21} = 0$. Figure 12 shows the augmented plant, P, which

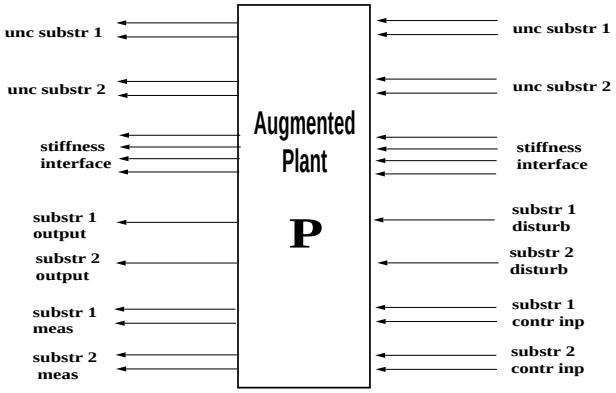

Figure 12: Augmented Plant for μ synthesis

includes all performance and uncertainty weights.

6.2.3 Design Weights for SRCP

For all cases, only the lowest 8 modes (16 states) for substructure 1 and lowest 4 modes (8 states) for substructure 2 are targeted for control while the rest of the component modes (32 and 16 modes for substructures 1 and 2) are treated as additive uncertainties. These are "normal" modes from substructure cantilever boundary conditions. No attempt is made to improve the reduced component modes (nominal) model by adding constraint modes or component shape functions to approximate the residual flexibility. As is typical of flexible structures, most higher frequency component modes are truncated. Figures 13 show the maximum singular value of the transfer function matrix of the truncated higher frequency component modes (solid) and a stable, real-rational, second-order weight function used as its upper bound (dotted) for both substructures. The weights representing upper bounds for substructure uncertainties have the realization:

$$W_1 = \left(\begin{array}{cc|c} -2.8622 & -7.5077 & -0.6458 \\ 7.5077 & -2.1794 & 0.4064 \\ \hline 0.6458 & 0.4064 & 0.0735 \end{array}\right) \quad (25)$$

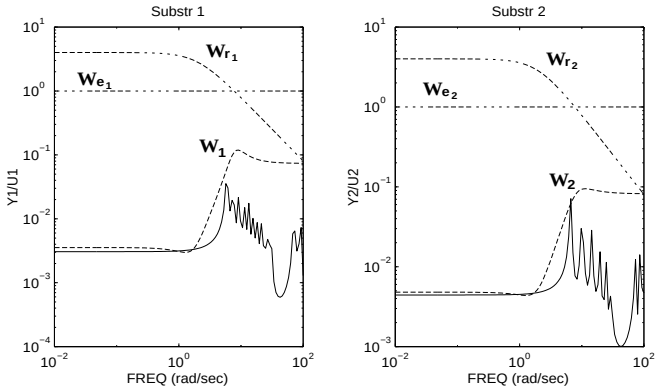

Figure 13: Substructure uncertainties and weights

$$W_2 = \left(\begin{array}{cc|c} -5.0127 & -7.1225 & -0.7768 \\ 7.1225 & -2.8930 & 0.3537 \\ \hline 0.7768 & 0.3537 & 0.0819 \end{array}\right) \quad (26)$$

The output weights, W_{e_1}, and W_{e_2}, (dash-dot) are chosen as unity. The figures also show a first-order frequency weighting function (dashed), W_{r_1}, W_{r_2}, where

$$W_{r_i} = \frac{s + 1000}{s + 2} * .008 \quad i \in [1, 2] \quad (27)$$

which is representative of the disturbance spectra at r_1 and r_2. They are chosen to reject external disturbances at lower frequencies (≤ 2 rad/sec).

6.3 Case Studies

Five cases are considered to illustrate the utility of the analysis and design framework based on substructure models as listed in Table 2. The cases are listed in

Case #	*Structure Interface*	*Controller*
1	$\gamma = 0,\ \alpha = 0$	$k_{12} = k_{21} = 0$
2	$\gamma = 1,\ \alpha = 0$	centralized
3	$\gamma = 1,\ \alpha = 0$	$k_{12} = k_{21} = 0$
4	$\gamma = 1,\ \lvert\alpha\rvert \leq 1$	centralized
5	$\gamma = 1,\ \lvert\alpha\rvert \leq 1$	$k_{12} = k_{21} = 0$

Table 2: Design configurations ($\beta = 1$)

increasing order of design difficulty. In this table, $\gamma = 0$ refers to zero nominal stiffness while α refers to the variation in the interface stiffness. The terms k_{ij}, $i, j \in [1, 2]$ refer to the controller component that maps the measured outputs from substructure j to control inputs of substructure i.

6.3.1 Uncoupled SRCP,$\gamma = \alpha = 0$ (Case 1)

This is the limiting case in performance and simplicity since the subsystems are completely uncoupled. The higher frequency truncated modes of the two substructures are the only model uncertainties assumed in this problem. The weighted frequency response plots in figures 14 show that disturbances are rejected very well at the low frequencies by two orders of magnitude over

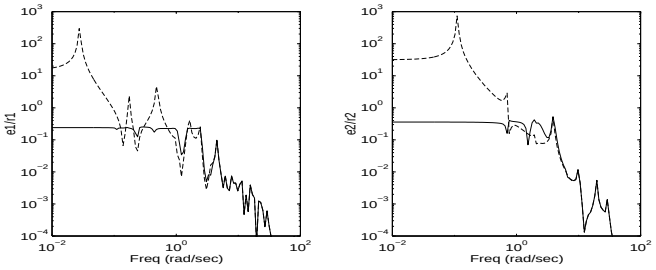

Figure 14: Frequency response for open loop (dotted) and closed-loop for controller 1 (solid), $\gamma = \alpha = 0$

the open loop response while avoiding spillover. The weighted open and closed loop frequency responses were calculated using the full model (80 and 40 states) for the substructures. Since the substructures are uncoupled ($\gamma = \alpha = 0$) and the controller is decentralized for this case, there is no cross coupling response. The figures also show a flat weighted closed-loop frequency response which is characteristic of optimal H_∞ controller response. In the transition bandwidths between the onset of performance rolloff ($\approx$ 2 rad/sec) and the onset of additive uncertainties ($\approx$ 7 rad/sec for substructure 1 and 2), rapid performance decay occurs.

6.3.2 Coupled SRCP, $\gamma = 1$, $\alpha = 0$ (Cases 2,3)

This configuration assumes a known fixed stiffness interface ($\gamma = 1$, $\alpha = 0$) between the two substructures. As in case 1, the higher frequency truncated component modes are the only model uncertainties assumed in this problem. The controller in case 2 is centralized while the controller in case 3 is decentralized. Only steps 1 and 2 of the sequential design was implemented for designing the decentralized robust controller in case 3. Controller order reduction at each step was done via balanced realization [35] for case 3.

Figure 15 shows the weighted closed-loop frequency responses from the combined disturbances to the outputs of interest when the structure is connected ($\gamma = 1$,$\alpha = 0$). A full model of the connected structure consisting of the first 30 modes were used in the open and closed loop frequency response. The open loop response (dotted) is shown for reference. At low frequencies, both controllers show excellent disturbance attenuation. Due to the controller constraint for case 3 (solid), a performance degradation is significant, especially in the transition bandwidth.

The closed loop response for the decentralized controller also show strong coupling between disturbances from one substructure to response of the other although the controller itself is uncoupled. This implies significant structural coupling as evidenced by the magnitude of the off-diagonal open-loop response. This is surprising since the nominal stiffness of the coupling section is two orders of magnitude less stiff than an equivalent length main substructure (see table 1). In fact, cantilever beams have large excitability and detectability at the free ends due to the dominating fundamental structural mode response. When the two free ends are connected, even with a "soft" interface stiffness, the system is highly coupled as just described. Therefore, although the relative numerical values of interface coupling stiffness may indicate weak coupling,

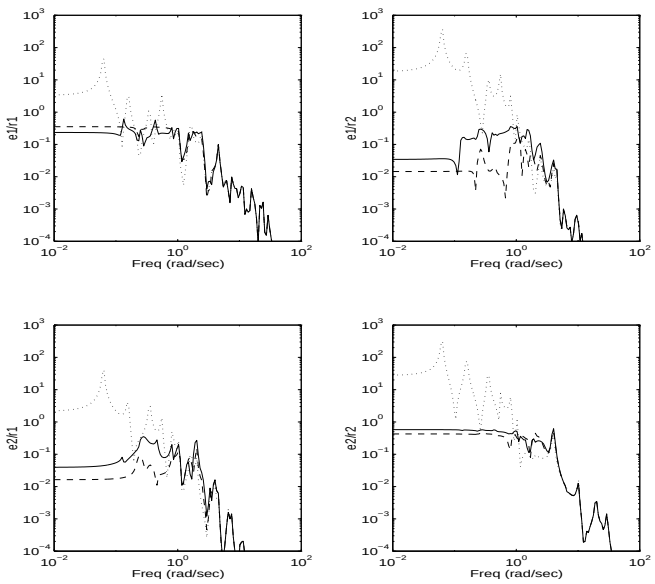

Figure 15: Frequency response for Cases 2 (dashed) and 3 (solid), $\gamma = 1$, $\alpha = 0$; open loop (dotted)

it is clear from the cross-terms that it is not for this particular example.

6.3.3 Coupled SRCP, $\gamma = 1$, $|\alpha| \leq 1$ (Cases 4,5)

This configuration is the same as cases 2 and 3 except that the substructure interface stiffness is assumed to be uncertain and/or variable over a known range ($|\alpha| \leq 1$). The uncertainty in the interface stiffness is assumed to vary about a nominal of $\gamma = 1$ which gives the nominal interface stiffness

$$s_o = \begin{bmatrix} -0.3 & -0.3 & 0.3 & -0.3 \\ -0.3 & -0.4 & 0.3 & -0.2 \\ 0.3 & 0.3 & -0.3 & 0.3 \\ -0.3 & -0.2 & 0.3 & -0.4 \end{bmatrix} \tag{28}$$

The nominal stiffness can be viewed as an intermediate stiffness condition between a fully coupled interface and where the two substructures are structurally uncoupled. From a physical standpoint, cases 4 and 5 are especially interesting because it covers the conditions before ($\alpha = -1$), during ($-1 < |\alpha| < 1$) and after ($|\alpha| = 1$) docking using fixed (spatially decentralized for case 5) controllers. Steps 1 to 3 of the sequential design was implemented for designing the decentralized robust controller in case 5. Controller order reduction at each step was also done via balanced realization.

Figure 16 shows the weighted frequency response at nominal stiffness where $\alpha = 0$. The open loop weighted frequency response (dotted) is also shown for reference. Both controllers 4 and 5 gives good disturbance rejection at low frequencies but at transient and higher frequencies, the decentralized controller significantly loses performance due to its controller constraint. The figure also show that the cross response (e_1/r_2 and e_2/r_1) is similar in magnitude to the local response (e_1/r_1 and e_2/r_2) even when the controller is decentralized for case 5.

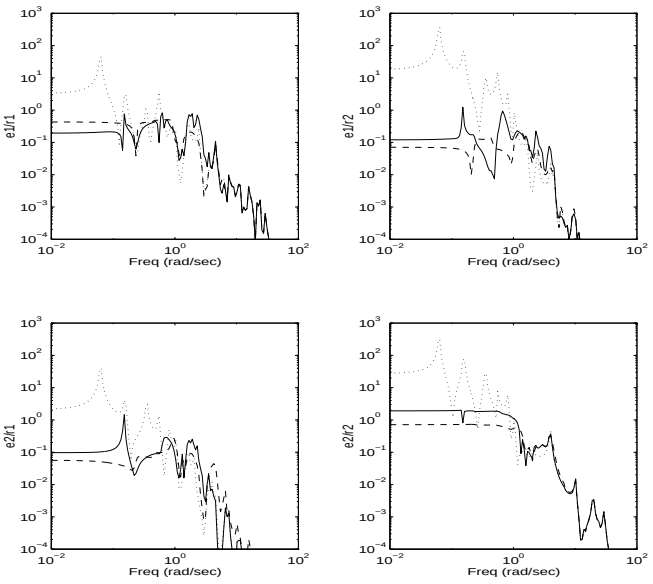

Figure 16: Frequency response for Cases 4 (dashed) and 5 (solid); open loop (dotted)

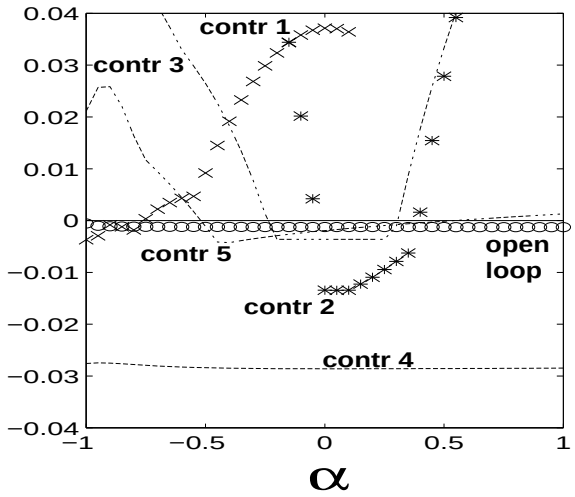

Figure 17: Variation in largest real component of closed loop eigenvalue with α; open loop (o), controller 1(x), 2(∗), 3(- -), 4($\cdots$), 5(- .)

6.3.4 Sensitivity to Interface Stiffness

The variations with α in the largest real component of the closed loop eigenvalues for all five controllers are shown in figure 17. A negative largest real component indicates stability and the figure shows the approximate range of interface stiffness variation over which the closed loop system remains stable using the evaluation model. Only controllers 4 and 5 are designed to accomodate specified variations in the interface stiffness. As expected, controller 1 (x) remains stable in a small neighborhood about $\alpha = -1$ when the substructures are completely uncoupled. Controller 2 (∗) remains stable in a small skewed neighborhood about $\alpha = 0$. Controller 3 (- -), which is the same as controller 2 except with decentralized control, gives a larger and more even neighborhood of stability than controller 2. Controller 4 ($\cdots$) is the only controller that guarantees robust stability over the whole range of α. With decentralization, controller 5 (- .) gives a smaller region of robustness than controller 4 but is still significantly larger than controllers 2 and 3.

Figure 18 shows the variation in the magnitude of the unweighted frequency response from input r_1 to output e_1 due to a change in interface stiffness for $\gamma = 1$, and $\alpha = (-.4, 0, .4)$. The open loop frequency response variation of the evaluation model is shown in figure 18(a) for reference. The changes in the interface stiffness significantly affect the frequency response of the structure over a wide frequency. Controller 1 was unstable for all three α values considered and is not shown. Controllers 2 and 3 were closed loop unstable at $\alpha = -.4$ and .4 and only the stable $\alpha = 0$ case is shown (dotted). Controllers 4 and 5 were closed loop stable for all three α values. This is not unexpected since they were the only controllers that accounted for the variation in the interface stiffness. Controller 4 gives the smallest variation (the three lines almost overlap) in the frequency response and is the most robust as expected.

Figure 19 show the dependence of the disturbance rejection performance (measured in terms of RMS error) on interface stiffness. The left, center, and right bar plot for each controller show the RMS value for $\alpha = -.4, 0, .4$, respectively. Unstable responses are denoted by 0.1 RMS error in the figure. The RMS errors for controllers 4 and 5 show only a small variation over the range of stiffness. There is a noticable drop in RMS performance for controller 5 due to controller decentralization. The nominal performance (at $\alpha = 0$) for controller 2 and 3 are slightly better than controller 4 and 5. This demonstrates the tradeoff in nominal performance for robustness over a larger set of structural configurations in the latter cases.

7 Concluding Remarks

There is currently no established means to quantitatively account for model errors or uncertainties for a set of reduced component mode models. In response, a modularized control design framework has been proposed such that substructure data can be utilized directly. This development could prove useful because it takes advantage of the existing significant body of results in substructure modeling of large flexible structures. Although substructure controllers are highlighted, centralized controllers can also be directly designed from substructure data. In addition, synthesis of the substructures, as is usually done in component modes synthesis, is not necessary for control design.

Although the numerical examples are based on a one dimensional structural system and is designed only to illustrate the proposed concept, it demonstrates a direct way to incorporate nominal substructure models and their corresponding uncertainties along with the substructure interface dynamics. The examples show that variations in the interface stiffness strongly affects stability and disturbance rejection performance. A small loss in nominal performance can be traded-off

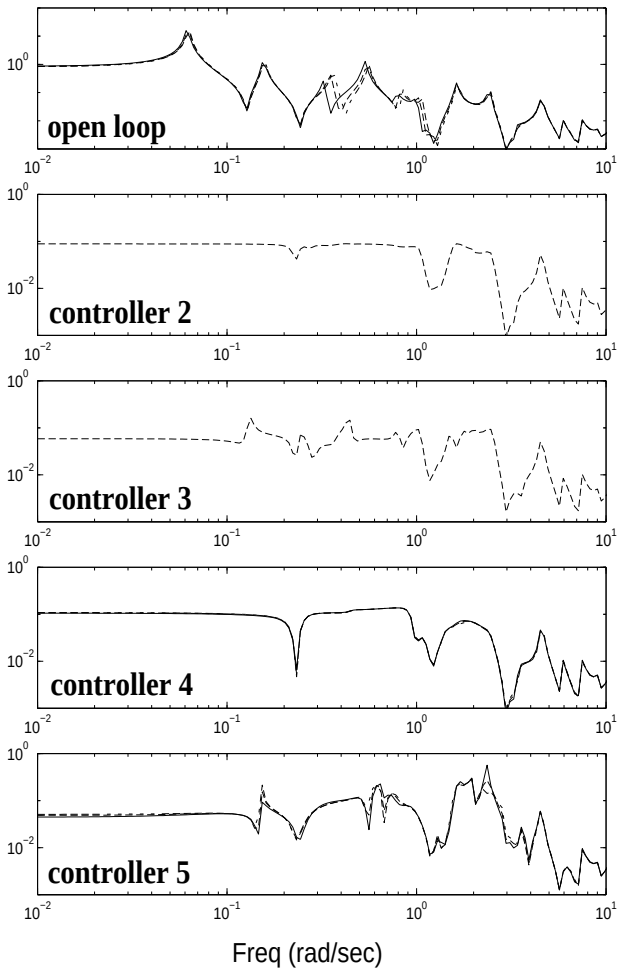

Figure 18: Variation in frequency response (e_1/r_1) with interface stiffness, $\gamma = 1$, $\alpha = -.4$ (solid), 0 (dotted), .4 (dashed)

for a significant gain in robustness. The results also demonstrate the feasibility of designing decentralized robust controllers by a sequential process although decentralization significantly reduced performance. Of course in the limiting case of uncoupled substructures, centralized controllers cannot be any better than decentralized controller.

Due to the 1-g testing environment, it may not be possible to test an assembled large flexible structure on the ground so that some comprehensive form of on-orbit system identification is critical. Since substructures can typically be tested independently in the laboratory, it is in principle possible to develop through testing component uncertainty models arising from inaccurate or reduced component modes and inconsistencies in the substructure boundary conditions. Perhaps the main advantage then in the proposed technique is in the reduction of the dependence on on-orbit system identification of the assembled structure by an easier and less costly testing of substructures on the ground. In addition, control designs that are based on a single model of the assembled structure cannot be experimentally validated on ground. These controllers would depend on nominal and uncertainty models that cannot be experimentally developed or validated.

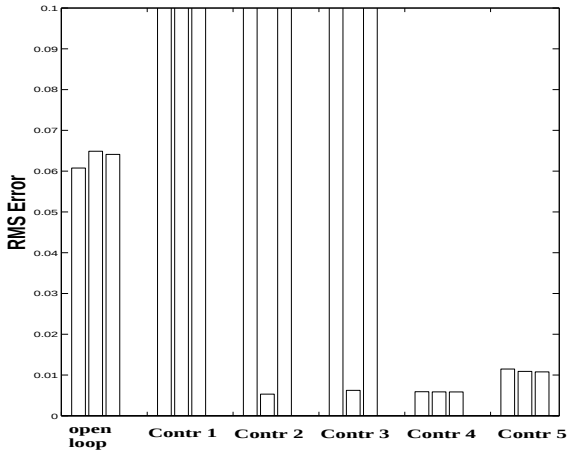

Figure 19: RMS error dependence on interface stiffness $\alpha = -.4$(left), 0(center), .4(right)

The technique is particularly suited for large, complex, flexible structures that are weakly coupled. The degree of weakness in the coupling should exceed a threshold such that its overall stability cannot be guaranteed if decentralized controllers are designed independently or if its adjoining substructures are accounted for inaccurately. In addition, performance limitations due to controller decentralization should be significant. In practice however, logistical constraints may make it impossible to implement a centralized controller.

Several important aspects of the coupled substructure robust control problem that are not adequately addressed and are open for further research include: modeling substructural interfaces beyond static stiffness, optimal substructure model reduction, role of errors in the low frequency modes of the subsystems, quantification of the degree of suboptimality of the decentralized design.

Acknowledgements

The author would like to thank the anonymous reviewers for their many valuable comments in the revision of this paper and D. Cox at NASA LaRC or his help with figures.

References

[1] Cooper, P.A., et. al, "Simulation of the Assembly Dynamics and Control of Space Station FREEDOM," AIAA Guidance, Navigation, and Control Conference, Monterey, CA, Aug 9-11, 1993.

[2] Garrison, J.L., Montgomery, R.C., Wu, S-C., Ghosh, D., and Demeo, M.E., "Space Shuttle to Space Station FREEDOM Berthing Dynamics Research at the NASA Langley Research Center,' *4-th Conf. on Intelligent Robotic Systems for Space Exploration* RPI, Troy, NY, Sept 30-Oct 1, 1992.

[3] Montgomery, R.C., et. al, "A Testbed for Research on Manipulator-Coupled Active Spacecraft," AIAA Guidance, Navigation, and Control Conference, Monterey, CA, Aug 9-11, 1993.

[4] Davison, E.J., "The Robust decentralized control of a general servomechanism problem," *IEEE Trans. on Auto. Contr.*, vol.,AC-21, No.1, Feb 1976, pp.14-24.

[5] West-Vukovich, G.S., and Davison, E.J., "The decentralized control of large flexible space structures," *IEEE Trans. on Auto. Contr.*, vol.,AC-29, No.10, Oct 84, pp.866-879.

[6] Davison, E.J., and Gesing, W., "Decentralized control of third generation spacecraft," *American Control Conference*, Minneapolis, MN, June 1987, pp.963-969.

[7] Joshi, S.M., *Control of Large Flexible Space Structures*, Vol.131 (Lecture Nores in Control and Information Sciences), Berlin: Springer-Verlag, 1989.

[8] Joshi, S.M., and Maghami, P.G., "Robust dissipative compensators for flexible spacecraft control," *IEEE Trans. on Aerospace and Electronic Systems,* vol.28, no.3, July 1992, pp.768-774.

[9] Vaz, A.F., and Davison, E.J., "The structured robust decentralized servomechanism problem for interconnected systems," *Automatica*, v.25, Mar. 89, pp.267-272.

[10] Young, K.D., "Distributed finite-element modeling and control approach for large flexible structures," *Journal of Guidance, Control, and Dynamics*, V.13, No.4, 1990, pp. 703-713.

[11] Su, T-J, and Craig, Roy R., Jr., "Substructural Controller Synthesis," 3rd Annual Conference on Aerospace Computational Control, Oxnard, CA, 1989.

[12] Su, T-J, "A Decentralized Linear Quadratic Control Design Method for Flexible Structures," Ph.D. Dissertation, The University of Texas, Austin, TX, 1989.

[13] Babuska, V., and Craig, R.R., Jr., "Substructure-Based Control of Flexible Structures," *AIAA 34th SDM Conference*, La Jolla, CA, April 1993, pp.3415-3422.

[14] Craig, R.R., Jr., and Bampton, M.C.C., "Coupling of Substructures for Dynamic Analysis," *AIAA Journal*, Vo.. 7, July 1968, pp. 1313-9.

[15] Craig, R.R., Jr., *Structural Dynamics - An Introduction to Computer Methods*, Wiley, New York, 1981.

[16] Meirovitch, L., *Computational Methods in Structural Dynamics*, Sijthoff & Noordhoof, Rockville, MD, 1980.

[17] Spanos, J.T. and Tsuha, W.S., " Selection of Component Modes for Flexible Multibody Simulation," *Journal of Guidance, Control, and Dynamics*, V.14, No.2, 1991, pp. 278-86.

[18] Lim, K.B., Maghami, P.G., and Joshi, S.M., "A Comparison of Controller Designs for an Experimental Flexible Structure," *IEEE Control Systems*, Vol.12, No.3, June 1992, pp. 108-118.

[19] Maciejowski, J.M., *Multivariable Feedback Design*, Addison-Wesley Publishing Company, Reading, MA, 1989.

[20] Doyle, J.C., "Analysis of Feedback Systems with Structured Uncertainties," Proc. IEE-D 129, 1982, pp. 242-250.

[21] Balas, G.J., and Doyle, J.C., "Robust Control of Flexible Modes in the Controller Crossover Region," *American Control Conference*, Pittsburg, PA, June 1989.

[22] Balas, G.J., Doyle, J. D., Glover, K., Packard, A. K., and Smith, R., *μ-Analysis and Synthesis Toolbox*, MUSYN Inc., Minneapolis, MN, 1991.

[23] Doyle, J.C., "Structured uncertainty in control system design," *IEEE CDC*, Ft. Lauderdale, December 85 (b).

[24] Bathe, K-J., *Finite element procedures in engineering analysis*, Prentice-Hall, Inc., Englewood Cliffs, New Jersey, 1982, Ch.8.

[25] Sandell, N.R., Jr., Varaiya, P., Athans, M., and Safonov, "Survey of Decentralized Control Methods for Large Scale Systems," *IEEE Transactions on Automatic Control*, Vol. AC-23, No.2, April 1978, pp.108-128.

[26] Mahmoud, M.S., Hassan, M.F., and Darwish, M.G., *Large-Scale Control Systems*, Marcel Dekker, Inc., New York, NY, 1985.

[27] Larson, R.E., McEntire, P.E., and O'Riley, J.G., *Distributed Control*, IEEE Computer Society Press, Silver Spring, MD, 1982.

[28] Doyle, J.C., Lenz, K., and Packard, A., "Design examples using μ synthesis: Space Shuttle Lateral Axis FCS during reentry," *IEEE CDC*, December 1986, pp.2218-2223; also in NATO ASI Series, vol. F34, Modelling, Robustness and Sensitivity Reduction in Control Systems, Ed. by R.F. Curtain, Springer-Verlag, 1987, pp.128-154.

[29] Packard, A., Doyle, J.C., and Balas, G.J., "Linear, multivariable robust control with a μ perspective," *ASME Journal of Dynamics, Measurements and Control Special Edition on Control*, vol.115, no.2b, June, 1993, pp.426-438.

[30] Stein, G., and Doyle, J.C., "Beyond singular values and loopshapes," *Journal of Guidance, Control, and Dynamics*, vol.14, no.1, 1991.

[31] Lim, K.B., and Balas, G.J., "Line-of-sight control of the CSI evolutionary model: μ Control," *American Control Conference*, Chicago, Ill, June 1992.

[32] Lim, K.B., and Cox, D.E., "Experimental robust control studies on an unstable magnetic suspension system," *American Control Conference*, Baltimore, Md, JLimune 29-July 1, 1994.

[33] Glover, K. and Doyle, J.C., "State-Space Formulae for all Stabilizing Controllers that Satisfy an H_∞ Norm Bound and Relations to Risk Sensitivity," *Systems and Control Letters*, vol. 11, pp. 167-172, 1988.

[34] Doyle, J.C., Glover, K., Khargonekar, P., and Francis, B., "State-space Solutions to Standard H_2 and H_∞ Control Problems," *IEEE Transactions on Automatic Control*, Vol.34, No.8, August 1989.

[35] Moore, B.C., "Principal component analysis in linear systems: controllability, observability, and model reduction," *IEEE Trans. on AC*, vol. AC-26, no.1, Feb. 81, pp.17-32.